08

Approach for obtaining Ge/Si(001) self-assembled hut wires for hole spin qubits

© D.V. Yurasov, M.V. Shaleev, A.V. Novikov

Institute for Physics of Microstructures, Russian Academy of Sciences, Nizhny Novgorod, Russia
E-mail: Inquisitor@ipmras.ru

Received July 4, 2025
Revised August 8, 2025
Accepted August 12, 2025

Method for fabrication of self-assembled Ge hut wires on Si(001) by molecular beam epitaxy is proposed. The approach is based on deposition of different amounts of Ge in two zones of a Si substrate and control of the surface morphology of one of the zones by reflection high-energy electron diffraction. It allows the deposition of a certain amount of Ge being arbitrarily close to the critical thickness of pseudomorphic growth in the second zone. Along with the optimized parameters of post-growth annealing, this allowed forming Ge hut wires with different parameters. Ge wires longer than $0.5\,\mu$m with low surface density were obtained, which are suitable for fabrication of hole spin qubits.

Keywords: SiGe heterostructures, molecular beam epitaxy, self-assembled islands, Ge hut wires.

DOI: 10.61011/TPL.2025.11.62211.20431

Various systems are currently being examined for their potential use in quantum computing: superconductors, trapped ions, semiconductors, photonic circuits, etc. [1]. Although semiconductors are still inferior to other material systems, their relatively easy scalability is an important advantage, which rests, among other things, on experience gained over many years of development of microelectronic technology. Si/Ge-based qubits are of the utmost interest, since they may be produced commercially. This heterosystem allows for construction of both electron and hole qubits. Research attention was focused on electron spin qubits at first, but hole qubits have a number of advantages [2]. Germanium nanowires (hut wires [2,3]) are a promising platform for the implementation of hole qubits. The possibility of self-assembly of Ge hut wires on a Si(001) surface by molecular beam epitaxy (MBE) without the use of catalysts has been demonstrated relatively recently [4,5]. It was found [4–6] that, within a narrow range of growth parameters, Ge hut wires may be formed from hut islands via diffusion of material from the wetting layer into islands during their long-term annealing in vacuum. Since the lateral faces of Ge hut islands are {105} planes and the Ge (105) plane has a low surface energy [7], the diffusing material is preferentially embedded in the „ends“ of hut islands, which leads to their elongation and the formation of hut wires with preservation of their height [4,6]. These hut wires are oriented along [100] or [010] crystallographic directions and are characterized by a uniform height and base width distribution.

One of the key issues associated with the formation of hut wires is the extreme narrowness of the range of growth parameters (the thickness of deposited Ge and the temperature of growth and subsequent annealing) that supports lateral elongation of the initially nucleated hut islands [6]. In view of this, an obvious requirement for their reproducible production is highly stable Ge evaporation source. Two types of such sources may be used in SiGe MBE setups: an electron beam evaporator (EBE) and an effusion cell. An EBE is the main option, since it is the only one to provide acceptable Ge deposition rates (~ 0.1 nm/s) and growth of structures of varying thickness (despite rate fluctuations due to mixing of convective flows of molten material). Although an effusion cell could provide a more stable material flow, it has significant drawbacks in regard to Ge evaporation. First, it needs to be heated to $> 1300\,^{\circ}$C, which is well above the melting point of Ge ($938\,^{\circ}$C), to reach even moderate Ge deposition rates (several hundredths of a nanometer per second). This is close to the operating temperature limits of pyrolytic boron nitride (PBN) crucibles typically used in cells ($T \sim 1400-1500\,^{\circ}$C). The process of thermal decomposition of PBN is already underway at such temperatures. Long-term exposure to high temperatures leads to PBN degradation and to doping of evaporated Ge with boron. Second, the temperature of a Ge cell needs to be reduced slowly in the process of cooling ($\sim 1-2\,^{\circ}$C/min), since Ge expands during crystallization, posing a risk of crucible destruction. Third, a PBN crucible needs to be replaced after several dozen Ge melting/crystallization cycles. Coupled with flow fluctuations during Ge deposition from an EBE, the narrow range of parameters within which hut wire formation is feasible makes it difficult to synthesize hut wires reproducibly. In the present study, we propose a method for controlled production of Ge hut wires with varying parameters with the use of an EBE as a deposition source. This method involves the formation of two Ge deposition zones on the substrate and monitoring of the surface state of one of the zones via reflection high-energy electron diffraction (RHEED).

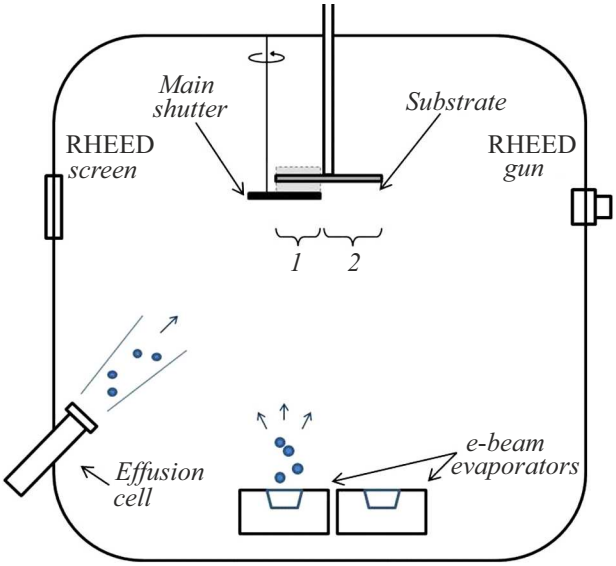

Figure 1. Schematic diagram of the growth chamber of the MBE setup with an effusion cell mounted at an angle to the substrate, EBEs mounted under the substrate, a substrate shutter, and a RHEED system. Numbers *1* and *2* denote different zones of Ge deposition (see text).

A Riber SIVA-21 MBE setup fitted with both an EBE and an effusion cell for Ge evaporation was used to grow the examined structures. To form Ge hut islands at temperature $T = 535\,^{\circ}\mathrm{C}$ with a low rate of ~ 0.005 nm/s (for both Ge sources), an amount of Ge slightly below the critical thickness of the 2D–3D transition was deposited (see below for more details). This was followed by annealing in the growth chamber at $T = 525\,^{\circ}\mathrm{C}$ for 2–4 h. The grown samples were studied using an NTEGRAPrima (NT-MDT) atomic force microscope (AFM) in the tapping mode. Figure 1 shows the schematic diagram of the growth chamber of the MBE setup (not all equipment is shown). With the used equipment, positioning of the effusion cell at an angle of $\sim 45^{\circ}$ to the substrate allows one to obtain a thickness gradient of deposited Ge on the order of $\pm 1\,\%$ at a distance of 1 mm from the wafer center.

Owing to a combination of this gradient and a narrow range of optimal thicknesses, the conditions necessary for the formation of hut wires are established only within a small section of the substrate, which was confirmed by AFM (Fig. 2). With a shift along the sample corresponding to a $\pm 5\,\%$ change in the amount of deposited Ge (± 0.25 of a monolayer (ML), where 1 ML ~ 0.14 nm; see Figs. 2, *a* and *c*) relative to the amount deposited in the center of the wafer (Fig. 2, *b*), the surface morphology changes greatly. Both relatively long low-density hut wires and significantly shorter wires with an order of magnitude higher density were obtained; an array of typical hut islands was also formed. However, the useful part of the sample containing hut wires with the required parameters is just a few mm^2 in size (i. e., corresponds to a very small fraction of the entire substrate). This makes it very hard to perform subsequent operations needed to produce electrostatic quantum dots and qubits based on them.

The method for controlled formation of hut wires with the use of an EBE (a Ge evaporation source typical for Si/Ge MBE) is implemented in the present study. The RHEED system allows one to determine the critical thickness of the 2D–3D transition in MBE (h_{crit}). However, if the material deposition is stopped at this point, islands with a fairly high density (more than $10^{10}\,\mathrm{cm}^{-2}$ for typical hut islands) will already be formed on the surface. Therefore, hut wires do not form upon further annealing of the sample, since free space for the expansion of hut islands in the lateral direction is lacking. Thus, to synthesize hut wires, one needs to deposit an amount of material that is slightly below h_{crit}. This amount cannot be determined *in situ* by analyzing the change in the RHEED pattern, since the diffraction pattern corresponds to two-dimensional growth if h_{crit} is not reached and the density of nucleated hut islands remains low. It is also hard to determine from calibration experiments due to the presence of fluctuations in the rate of Ge evaporation from the EBE. To find the required amount of deposited Ge, we propose dividing the Si substrate into

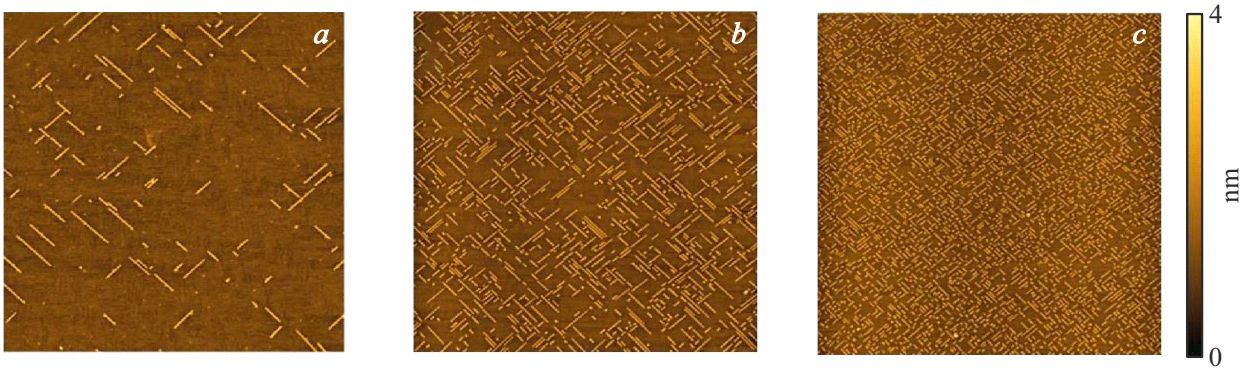

Figure 2. AFM images of different regions of the sample grown with a thickness gradient of deposited Ge: *a* — shifted away from the center by a distance corresponding to a 0.25 ML reduction in the amount of Ge relative to that at the center; *b* — center of the sample; *c* — shifted away from the center by a distance corresponding to a 0.25 ML increase in the amount of Ge. All scans are $3 \times 3\,\mu$m in size.

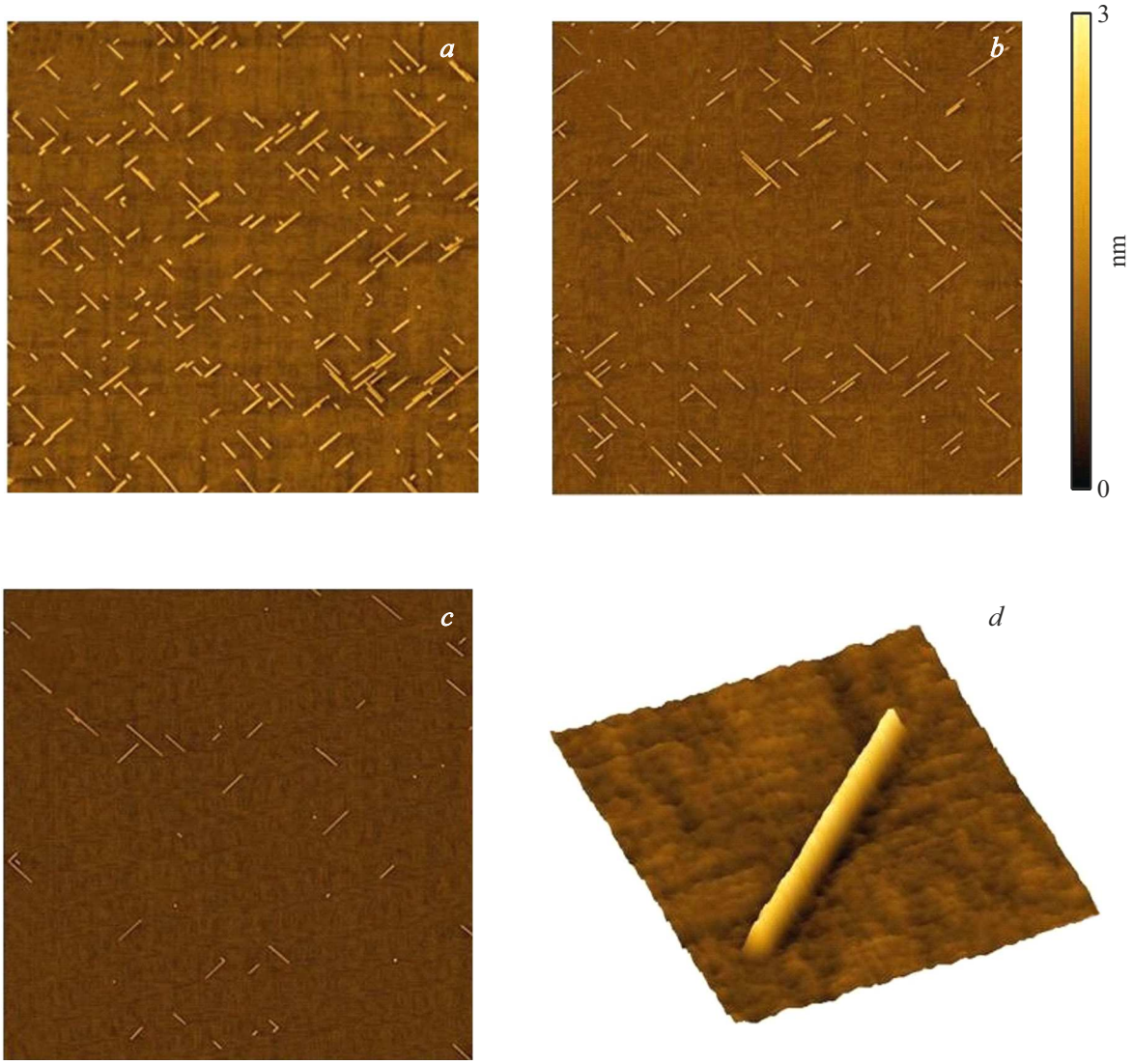

Figure 3. AFM images of structures (in zone *1* in Fig. 1) fabricated using the EBE in accordance with the proposed procedure. The magnitude of detuning from the critical thickness Δh is 0.35 (*a*), 0.43 (*b*), and 0.5 ML (*c*). All scans are $5 \times 5\,\mu$m in size. *d* — 3D AFM image of an individual hut wire; the scan is $0.5 \times 0.5\,\mu$m in size.

two zones that differ in the amount of Ge. A certain amount of Ge (Δh) is first deposited only on zone *2* (Fig. 1), while the other part of the substrate is shielded by a shutter (zone *1* in Fig. 1). This shutter is a standard component that is typically present in MBE chambers. Following the deposition of a Ge layer with thickness Δh, the shutter is opened, and Ge is deposited on the entire substrate up to the moment when the transition to island growth in zone *2* is observed in the RHEED pattern. The total thickness of deposited Ge in zones *2* and *1* is then $h_2 = h_{crit}$ and $h_1 = h_{crit} - \Delta h$, respectively. In this case, typical high-density hut islands always form in zone *2*, while zone *1* features (if Δh was chosen correctly) sparse hut islands that have enough space for elongation and may form hut wires during annealing. The relative error due to Ge flow fluctuations is thus reduced manyfold, since variations of the amount of deposited Ge affect primarily the value of Δh, which is many times smaller than h_{crit}. One may adjust the thickness detuning from h_{crit} in zone *1* of the substrate and control the parameters of the resulting hut wires by varying Δh. In this case, the area of the substrate region suitable for hut wire formation may be many times larger than the one found in experiments on Ge evaporation from an inclined source.

The approach described above was used to produce samples with different values of detuning $\Delta h \sim 0.35{-}0.5$ ML ($h_{crit} \approx 5.3$ ML). The temperatures set for growth and post-growth annealing (2–4 h) were $T = 535\,^{\circ}$C and $T = 525\,^{\circ}$C, respectively. To prevent oxidation, hut wires were overgrown with a 3-nm-thick Si layer at $T = 300\,^{\circ}$C [4]. Figure 3 shows the AFM images of the obtained samples. At $\Delta h = 0.35$ ML (Fig. 3, *a*), short hut wires 200–350 nm in length with a density of $\sim 10^9$ cm^{-2} were formed on the surface. With Δh increased to 0.43 ML,

the density of hut wires dropped to $\sim 6 \cdot 10^8\,\mathrm{cm}^{-2}$, while their length increased to 300–500 nm (Fig. 3, *b*). At $\Delta h = 0.5$ ML, rather sparse hut wires with a density of $\sim (1-2) \cdot 10^8\,\mathrm{cm}^{-2}$ and a length up to 600 nm formed on the surface (Fig. 3, *c*). Figure 3, *d* shows an individual hut wire. In all cases, their height was ~ 1.5 nm, which corresponds to the data reported in [4–6]. A length on the order of 500 nm is sufficient to perform further technological processing of an individual hut wire for qubit formation [6,8].

Thus, the proposed approach makes it possible to form Ge hut wires with controlled parameters using an EBE as a Ge evaporation source typical for Si/Ge MBE setups and a method for depositing different amounts of Ge on two zones of a substrate. The useful area on which Ge hut wires are synthesized may constitute a fairly large fraction of the total area of the substrate. These structures may be used to form hole spin qubits, possibly with longer coherence times achieved through the application of materials with a reduced concentration of ^{29}Si and ^{73}Ge isotopes with a non-zero nuclear spin [9].

Funding

This study was carried out under the state assignment of the Institute of Physics of Microstructures of the Russian Academy of Sciences (FFUF-2024-0019).

Conflict of interest

The authors declare that they have no conflict of interest.

References

[1] N.P. de Leon, K.M. Itoh, D. Kim, K.K. Mehta, T.E. Northup, H. Paik, B.S. Palmer, N. Samarth, S. Sangtawesin, D.W. Steuerman, Science, **372**, eabb282 (2021). DOI: 10.1126/science.abb2823
[2] G. Scapucci, C. Kloeffel, F.A. Zwanenburg, D. Loss, M. Myronov, J.-J. Zhang, S. De Franceschi, G. Katsaros, M. Veldhorst, Nat. Rev. Mater., **6**, 926 (2021). DOI: 10.1038/s41578-020-00262-z
[3] H. Watzinger, J. Kukucka, L. Vukušić, F. Gao, T. Wang, F. Schäffler, J.-J. Zhang, G. Katsaros, Nat. Commun., **9**, 3908 (2018). DOI: 10.1038/s41467-018-06418-4
[4] J.J. Zhang, G. Katsaros, F. Montalenti, D. Scopece, R.O. Rezaev, C. Mickel, B. Rellinghaus, L. Miglio, S. De Franceschi, A. Rastelli, O.G. Schmidt, Phys. Rev. Lett., **109**, 085502 (2012). DOI: 10.1103/PhysRevLett.109.085502
[5] J.J. Zhang, A. Rastelli, O.G. Schmidt, D. Scopece, L. Miglio, F. Montalenti, Appl. Phys. Lett., **103**, 083109 (2013). DOI: 10.1063/1.4818717
[6] J. Aberl, L. Vukusic, F. Fournel, J.-M. Hartmann, M. Brehm, Phys. Status Solidi A, **219**, 2200145 (2022). DOI: 10.1002/pssa.202200145
[7] G.H. Lu, M. Cuma, F. Liu, Phys. Rev. B, **72**, 125415 (2005). DOI: 10.1103/PhysRevB.72.125415
[8] K. Wang, G. Xu, F. Gao, H. Liu, R.-L. Ma, X. Zhang, Z. Wang, G. Cao, T. Wang, J.-J. Zhang, D. Culcer, X. Hu, H.-W. Jiang, H.-O. Li, G.-C. Guo, G.-P. Guo, Nat. Commun., **13**, 206 (2022). DOI: 10.1038/s41467-021-27880-7
[9] D.V. Yurasov, A.V. Novikov, M.V. Shaleev, M.N. Drozdov, E.V. Demidov, A.V. Antonov, L.V. Krasilnikova, D.A. Shmyrin, P.A. Yunin, Z.F. Krasilnik, S.V. Sitnikov, D.V. Sheglov, Tech. Phys. Lett., **50** (5), 56 (2024). DOI: 10.61011/TPL.2024.05.58424.19813.

Translated by D.Safin